# Attributes of Two Dimensional Magnetic Self-Assembly

Shuhei Miyashita[1] and Rolf Pfeifer[2]

[1]NanoRobotics Lab.

Department of Mechanical Engineering

Carnegie Mellon University

5000 Forbes Ave, Scaife Hall 423

Pittsburgh, PA 15213

+1 412 2288008

shuheim@andrew.cmu.edu

[2]Artificial Intelligence Laboratory

Department of Informatics

University of Zurich

Andreasstrasse 15, 8050 Zurich

Switzerland

**Abstract**

Self-assembly is a phenomenon broadly observed in nature where a vast number of various molecules spontaneously synthesize complex structures. In this paper, prompted by the need for the realization of highly autonomous self-assembly systems that employ magnetism as a driving force, we discuss fundamental issues associated with magnetically driven self-assembly systems. We first introduce some examples from our case studies, in which the models all subscribe to a distributed approach, and thus lack central control. Then we categorize them by their type of magnetic attachment. The discussed issues include several fundamental properties, such as the effect of morphology, stochasticity, the difference between 2D models vs. 3D models, emergence, allostericity, and parallelism. The obtained conclusions support our stance that the appropriate morphology lightens the control cost for the assembly, providing primal but engaging instances of magnetic self-assembly systems that warrant further study.

keywords

self-assembly, morphology, magnetism, embodiment, autonomous distributed system

# 1 Introduction

Microbiological discoveries in the last several decades have provided an accurate and enhanced view of nature. An exemplary feature is that the components of the main constituent, such as proteins, spontaneously synthesize within organisms and maintain formed structures through an intricate web of intra-molecular interactions. These types of distributed bottom-up processes often enable the subject to attain robust features, such as morphogenesis, self-repair, or metabolism. This fact has inspired engineers to anticipate innovative products, in the form of self-repairable machines, which are efficient at attaining equivalent capabilities.

Half a century ago, even before the realization of the tremendous challenge of constructing self-assembling machines in the 1990s, some pioneering work had already been executed. Efforts were begun to abstract higher-level design principles to clarify the actual dynamic processes underlying these interactions. Penrose presented a provoking self-replication model that was mechanically realized (Penrose, 1959, 1958). This work was followed by several studies that focused on elements, such as clustering patterns of passive elements and investigating the role of shape on templates and components (Cohn and Kim, 1991; Breivik, 2001). A simple but elegant design was demonstrated by Hosokawa, in which the components could react to an input and allow new bondings (Hosokawa et al., 1994). Notable ideas about conformational switch were proposed by Saitou and Jakiela *et al.* (Saitou, 1999; Saitou and Jakiela, 1995b,a; Saitou et al., 2000), although his work represented more conceptual demonstrations for theoretical justifications. A series of studies were conducted by Whitesides et al. to realize the positional coordinates of molecule-mimetic chemistry (Bowden et al., 2001, 1997; Grzybowski et al., 2003; Wolfe et al., 2003), circuit functionality (Gracias et al., 2000; Boncheva et al., 2002, 2003), reversible aggregation (Mao et al., 2002), folding structures (Boncheva et al., 2005), the rotation of magnets (Grzybowski et al., 2000), and the rotation of rotors (Grzybowski et al., 2004). Similarly, numerous research efforts have been devoted to the investigation of morphology (Stambaugh et al., 2003). Artificial chemicals that can form in several ways depending on the temperature of the system, such as polymers and dimers, were demonstrated in (Breivik, 2001). Different aggregation patterns with various sizes of components were shown in (Yamaki et al., 1995). An intelligent self-assembling block that can represent multiple states by the units' rotational angle was designed by (Tsutsumi and Murata, 2007). The system can physically conduct XOR calculation on a 2D plane. These self-assembly blocks can be categorized into two types: those that are passive and those that have states that regulate their bindings. All these models are simple enough to be scaled down (realized on the physical level). Yet few of the models attained "functionality" of the compound, such as in an electric circuit. Also, these models presumed environmental turbulence as the driving force of the reactions (not self-propulsion), which is a reasonable premise when the module size is small enough.

Another trend was adopted from robotics. These modules are settled on a ground with low friction and

agitated to achieve locomotion. The method of agitation varied: the use of an air-table with mechanical turbulence (White et al., 2004), air-jet turbulence (Klavins, 2007; Bishop et al., 2005; Griffith et al., 2005), or fluid turbulence (White et al., 2005; Tolley and Lipson, 2010). Some have a unique characteristic, such as morph by disassembly (Gilpin et al., 2010). Yokoi *et al.* adopted robotic and chemical approaches in which he developed a physically connected multi-robot system and a system that could control a drop of mercury (Yokoi et al., 2003). A good review article surveying this field was published by Gross and Dorigo (Gross and Dorigo, 2008).

To our knowledge, few artificial self-assembly systems with *mm* to *cm* scales have attained spontaneous aggregation with intrinsic driving mechanisms. In other words, existing approaches require accompanied driving force for interactions such as air flow or fluid flow, in addition to magnets for docking mechanisms. Despite the ubiquitous nature of the force exertion and the ideal scalability of magnetism, few successful attempts have been made to employ magnetism in the context of artificial self-assembly. In this paper, motivated by the potential of magnetism in driving mechanisms of artificial self-assembly systems, we summarize our exploratory study that included a series of experiments and provide an integrated view of design issues related to the magnet-based self-assembly systems. We further survey relevant issues and discuss them based on the obtained results. The paper is organized as follows. In Section 2, we describe the experimental setup. In Section 3, we present various experimental results by classifying them into several groups according to the assembly patterns. This is followed by a discussion in Section 4 in which we raise and summarize relevant issues discovered through the process. Finally, Section 5 concludes the paper.

## 2 Experimental Setup

The term self-assembly implies a notion in which components rove around the environment and spontaneously compose structures. The processes are normally realized in a distributed and stochastic manner, that is, once a set of experimental conditions is invoked, components act in parallel, intrinsically following local causal rules imposed by the system. Inspired by various instances that demonstrate self-assembly in nature, we have constructed an experimental platform to analytically investigate the properties of self-assembly (Miyashita et al., 2008a, 2011).

[Figure 1]

The platform was simple, but sufficient to study the relation of magnetism, morphology, dynamics, and the product yield of a system. The main attributes of the platform are: magnet driven, stochastic, distributed and scalable (Miyashita et al., 2011). The experimental apparatus consisted of centimeter-

sized floating modules, a water container, a pantograph mechanism, and a power supply. We prepared three types of modules: passive (Figure 1 (i)), self-agitative (Figure 1 (ii)), and manually fixed position (Figure 1 (iii)). All types had a single permanent magnet at the bottom for attaining attractive/repulsive interactions. The magnets were attached either horizontally or vertically, depending on the experiment (Figure 1 left-bottom illustration). Passive elements had no motors; they were simply floating tiles with an attached magnet. A self-agitative module and a manually handled module featured flat coreless vibration motors (T.P.C FM34F, $12000 \sim 14000\,rpm\,(2.5-3.5\,V)$, vibration quantity $17.6\,m/s^2$), which were directly attached on their bodies (Figure 1 photo). This allowed the modules to jiggle and rove around on the water. As a power supply for the modules with vibration motors, we opted to supply electricity through a pantograph that drew current from a metallic ceiling (Figure 1). When voltage (E) was applied to the ceiling plate, current flowed through the pantograph to the vibration motor on a module, returning to ground via electrodes immersed in the conductive water (NaCl solution, $83.3\,g/l$). This mechanism enabled all the (ii) and (iii) type modules to acquire the same voltage. Since the rotational speed of the eccentric mass in a vibration motor is approximately proportional to the voltage applied, the voltage can be used as the magnitude of agitation (temperature at the macro scale). As the speed increases, it leads to faster movement of the modules and stronger collisions between them. The chemical reaction $2\mathrm{NaCl} + \mathrm{H_2O} \rightarrow \mathrm{H_2} \uparrow + \mathrm{Cl_2} \uparrow + 2\mathrm{NaOH}$ occurs in the NaCl solution to run the current, and the concentration sufficiently sustains the current flow during the entire course of the experiment. Platinum was selected for the electrode to avoid chemical deposition. A camera was set below the transparent container to observe the experiments.

Given $N$ as the number of permanent magnets existing in the system, the magnetic force ($\boldsymbol{F}_{ij}$) and the magnetic torque ($\boldsymbol{\tau}_{ij}$) experienced by $i$-th magnet by interacting with $j$-th magnet ($i, j \in \mathbb{N}$) can be expressed and simplified as:

$$\boldsymbol{F}_{ij} = \mu_0 \int_{vi} (\boldsymbol{M}_i \cdot \nabla)\, \boldsymbol{H}_j \, dv \approx \mu_0 v_i (\boldsymbol{M}_i \cdot \nabla) \boldsymbol{H}_j \tag{1}$$

$$\boldsymbol{\tau}_{ij} = \mu_0 \int_{vi} (\boldsymbol{M}_i \times \boldsymbol{H}_j)\, dv \approx \mu_0 v_i \boldsymbol{M}_i \times \boldsymbol{H}_j \tag{2}$$

where $\boldsymbol{H}_j$ is the magnetic field exerted by $j$-th magnet, $\mu_0 = 4\pi \times 10^{-7}$ (Tm/A) is the permeability of free space, $v_i$ and $\boldsymbol{M}_i$ are the volume and the magnetization of $i$-th magnet, respectively.

The magnetic field created by $j$-th magnet with respect to the position $\boldsymbol{r}$ can be described as

$$\boldsymbol{H}_j(\boldsymbol{r}) = \frac{1}{4\pi|\boldsymbol{r}^3|}\Big(\frac{3(v_j \boldsymbol{M}_j \cdot \boldsymbol{r})\boldsymbol{r}}{|\boldsymbol{r}|^2} - v_j \boldsymbol{M}_j\Big). \tag{3}$$

Utilizing $\boldsymbol{H}$, the total magnetic potential energy of the system ($U_{total}$) can be described as

$$U_{total} = -\frac{\mu_0}{2} \sum_{i,j\ i\neq j}^{N} \int_v \boldsymbol{M}_i \cdot \boldsymbol{H}_j \, dv. \tag{4}$$

In general, magnetic force decays in inverse proportion to distance to the power of four ($\propto r^{-4}$), torque and energy to the power of three ($\propto r^{-3}$). Systems consisting of permanent magnets act to minimize the magnetic potential energy over time.

# 3 Classification of Assembly Patterns

In this section, we present the assembly patterns formed by differently shaped modules. The observed behaviors are shown in Figure 2 and Figure 3, in which the magnets are horizontally attached (in Figure 2), or vertically attached (in Figure 3). Some are powered via the ceiling plate (Figure 2 ,(b), (c), (d), Figure 3 (g)), while the others are powered through a wire being sustained by hand (Figure 3 (h), (i)), passive but externally agitated (Figure 3 (f)), or pure passive (Figure 2 (a), Figure 3 (j), (k)). Note that these self-assembly processes occur without any centralized controls. We set the following categorization for the displayed outcomes: outcomes that are physically demonstrated within a set of conditions (Figure 3 (h),(i)), outcomes that are tested in experiments (Figure 2 (a)-(e), and Figure 3 (g)), outcomes that are surveyed within a statistical study (Lattice (Figure 3 (f)), Mobility (Figure 3 (g)), and Logical reactions (Figure 3 (j),(k))). All the results are confirmed based on these criteria.

## 3.1 Horizontal magnetic alignment

In Figure 2, five aggregation patterns are presented in which the magnets are horizontally attached to the modules (see Figure 1). The initial and the final configurations are presented, respectively, next to the modules' schematic illustrations with their magnets' attachments.

[Figure 2]

We classified the observed assembly patterns into two groups: namely, Linear alignment, Clustering, and Tree, according to the topology created. The representative states of modules and clusters can be described with chemical symbols, such as $\mathcal{A}_\cdot, \mathcal{B}_\cdot$, or $\mathcal{C}_\cdot$, where $\mathcal{A}$, $\mathcal{B}$, and $\mathcal{C}$ are modules/clusters and $\cdot$ denotes the number of constituents ($k, l, m, n \in \mathbb{N}$).

- Linear alignment ($\mathcal{A}_k$)
  - **Figure 2 (a): A set of rectangular modules aligns into a straight configuration.** Each module contains a horizontally attached magnet directing to the long edges. The torque that

acts proportional to the distance of the order of three ($\propto r^{-3}$) induces a quick turn of the modules and causes them to attach along the long edges.

- Clustering ($m\mathcal{A}_k$)
  - **Figure 2 (b): Circular modules form dimers.** Magnets attached between the center and the end of each module cause the formation of a pair, impeding the attachment of a third module.
  - **Figure 2 (c): Kite-shaped modules configure trimers.** Similar to (c), modules with magnets attached at the obtuse corner gather together facing the corners. Note that the other formation, three 2-clusters, can be formed with a fixed number of six modules.
  - **Figure 2 (d): Six circular cut-shaped modules form a circle.** Similar to (d), magnetic flux is "closed" by the modules occupying the space for possible attachment. Note that providing a greater number of modules does not guarantee that full circle configurations will be producedMiyashita et al. (2011).
- Tree ($m\mathcal{A}_k\, n\mathcal{B}_l$)
  - **Figure 2 (e): Triangular modules configure a tree formation.** The modules in which the north poles of the magnets pointed to the tips of the triangles create a branching formation.

The system shows the characteristics of monopoles due to the arrangement of the magnets.

## 3.2 Vertical magnetic alignment

Figure 3 shows six assembly patterns that are obtained by attaching the magnet vertically to the modules' bottom surface.

[Figure 3]

In each example, a schematic is presented with the orientation of the magnets' attachment, and the initial and final configurations with snapshots. The assembly patterns are classified into two folds: alternate positioning and logical reaction.

- Alternate positioning ($(\mathcal{AB})_k$)
  - **Figure 3 (f): Passive square modules form lattice structures.** Square modules with a magnetic north pointing upward (red modules) and those with a magnetic south pointing upward (white modules) produce a lattice structure. The system is pure passive, externally agitated, and can even attain repulsion among modules, depending on the configurations (see (Miyashita et al., 2009b)).

- **Figure 3 (g): Vibrating triangular module and circular modules induce translative wheeling action.** A vibrating triangular module with a magnetic north pointing upward attracts circular modules with magnetic south pointing upward. Due to the rotational torque induced by a vibration motor implemented on the triangular module, rotational and translative motions are imposed on the group (Miyashita, 2011).
- **Figure 3 (h): Vibrating and passive circles configure a concentric circle.** Mutual attraction occurs between the large module at the center and the small modules around it, while the small modules repel and stay apart from one another. The vibration of the large module forces the small passive modules to rotate around themselves. At the same time, the small modules individually rotate on site in the opposite direction (Miyashita et al., 2009a).
- **Figure 3 (i): A simple gear system is created by a vibrating triangle and passive circles.** This example demonstrates that the torque induced by a vibrating module (triangular module not fixed) can be transferred through a set of passive circular modules.

• Logical reaction ($\mathcal{A} + \mathcal{B} + \mathcal{C} \rightarrow \mathcal{AC} + \mathcal{B} \rightarrow \mathcal{ABC}$)

- **Figure 3 (j): Logical enzyme reactions can be realized by passive modules.** A module mimicking enzyme function acts on substrate modules. Here all the modules are passive. The small circular module attaches to the large module, causing a conformation change(i.e., the release of a magnet from the large module). This causes the small square module and the catalyzing circular module to be released (Audretsch, 2009).
- **Figure 3 (k): A third module can cause disassembly.** A module releases a part of its body by connecting to another module, which again causes conformation change (by sliding the position of the magnet within the body) (Audretsch, 2009). All the modules are passive.

These assemblies show the characteristics of dipoles, and the representative assembly patterns are alternate positioning.

## 3.3 Properties

Table 1 lists the properties attributed to the particular configurations shown in Figure 2 and Figure 3, respectively.

[Table 1]

1. **Reaction.** All the assembly processes shown can be examined in relation to chemical reactions, and hence are described by chemical formulae. Some confrontational notions in chemistry, such as *elements/compounds* or *reactants/products*, can also be adopted at this scale. *Stoichiometric*

*coefficients* exist and can be derived from the respective reactions. The performances of assembly can be assessed using the *yield rate*. However, there are some notions that cannot easily be adopted, such as *temperature* or *pressure*. Moreover, definitions of physical phases, such as *gas* or *liquid*, at this scale require further clarification.

2. **Product.** The obtained products can be categorized into two groups: those that are open to further growth (polymer) and those that are closed (clusters). The possibility for further growth corresponds to the states of magnetic fluxes. That is, polymers, lattices, and concentric circles are capable of continuing to grow so long as additional modules are supplied; dimers, trimers, and hexamers are restricted from developing further.

3. **Magnetic flux.**

   Horizontal magnetic alignment and vertical magnetic alignment have different customs on flux capturing. Figure 4 shows the distribution of the norms of magnetic flux density $||B||$ (we set the magnetization of each magnet as 750 [kA/m]) when four magnets are horizontally attached ((a) in top view and (b) in side view) and vertically attached ((c) in top view and (d) in side view) in a lattice structure. We calculated the value with the finite element method using software available in the market (COMSOL). The norms of magnet flux density spread similarly in horizontal directions (indicated as $L_1$), whereas they spread differently in vertical directions ($L_2 < L_3$). This means that the flux is more open to the vertical axis when using vertical alignment. Using horizontal alignment, magnetic flux can be more easily "closed" to the exterior by magnets filling the space where the flux goes.

[Figure 4]

4. **Structural isomer.** Although the obtained assembly patterns are typical outcomes that we obtained with the described settings, this does not mean that these are the only outcomes possible with the given configurations. For example, structural isomers, which are different configurations consisting of the same set of modules, exist in many cases (e.g., Figure 2 (e), Figure 3 (f)). In our experience, the topologies formed received little influence from experimental conditions, such as initial positions or module density. The magnetically stable states can be compared using magnetic potential energies. The example shown in Figure 3 (i) is in this sense unstable; more stable isometric configurations exist, hence modules are manually supplied at the end of the alignment.

5. **Functionality.** Some particular configurations show a correspondence between shape, behavior, and function. These functions are often obtained as emergent behaviors that are intrinsically comprised. Most of the assemblies show mere spacial patterning.

6. **Controllable parameter.** The interactions occur locally, although some global parameters exist, such as the level of agitation of the water container or the applied voltage. All these variables may give rise to different aggregation patterns.

7. **Dynamics.** A dynamical equilibrium state represents one of the unique characteristics of dynamical systems, which show certain (in)stabilities in their intrinsic dynamics. Dynamically stable states show different characteristics from statically stable states. The formed structure can exist only by consuming energy and often shows robustness against external turbulence. We want to draw special attention to Figure 3 (g), in which the compound acquires mobility function. In general, compared to traditional pick-and-place style assembly processes, a narrower range of assembly freedoms are given to the system and it produces a semi-particular product.

8. **Self-repair.** Homogeneous systems, such as biological organisms, commonly consist of homogeneous cells and thus feature redundant properties. The observed assembly processes and the configurations are typically robust against unforeseen damage, implying that the system could recover from failures and external disturbances to some degree (self-repairable). The possibility for self-repair can be discussed by analyzing the second derivative of magnetic potential energy by slightly deflecting the positions of constituent modules for $\Delta x$.

Table 2 summarizes the features of horizontal and vertical magnetic attachments. Horizontal alignment is suitable when employing controllable torque in the system. However this implies that, due to the strong magnetic torque causing an instant rotation of modules, repulsion can only be introduced by environmental turbulence; it is difficult to do by magnetism. Hence, regardless of the module's shape, the system shows aspects of a homogeneous system in its assembly. On the contrary, vertical alignment can be treated as a monopole model. This lightens the burden of designing the system. However, this also acts as a disadvantage because the system cannot exploit strong torque when necessary. Moreover, it is difficult to close the flux, which means halting the assembly requires a specific treatment.

[Table 2]

The characteristic of vertical attachment is that repulsion and attraction can naturally co-exist in the system. Hence this type of magnet's arrangement is appropriate for complex models, such as in Figure3 (j), (k). It has to be added that geomagnetism affects horizontal alignment on their orientations.

# 4 Discussions

In this section, we discuss subjects attributed to self-assembly systems that specifically employ magnetism as the main driving force for the assembly from three perspectives; namely (1) shape, (2) assembly issue,

and (3) environmental issue (Figure 5).

[Figure 5]

## 4.1 Shape

In nature, morphology plays a crucial role in self-assembly systems. The presented demonstrations imply that an essential role is often played by the distribution of the body parts from the "origin of the force" (i.e., the magnets) rather than the overall geometry. A practical approach is to evaluate shape from an energetic perspective, and develop a scheme to ground the phenomenon in the context of physics.

[Figure 6]

### 4.1.1 Horizontal alignment

Modules having convex shapes can uniquely be described as a function of two variables: the distance from the origin of the force to the edge ($r$) and its angle from the initial contact point ($\theta$) (termed *shape function*, Figure 6). In the case of horizontal magnet alignment, aggregation patterns are mainly influenced by the four edge positions at angles 0, $-\frac{\pi}{2}$, $-\frac{\pi}{2}$, and $\pi$ (Figure 6 (a)). If the edge angles at 0 and $\pi$ are positive to the increase of $\theta$ (i.e., $\frac{dr}{d\theta}|_{\theta=0,\pi} > 0$), the module tends to acquire another module on its left side, eventually forming a global pattern curving toward left, and vice versa (c.f., Figure 2 (c) and (d)). If the shape is symmetric, that is, $r|_{\theta-\Delta\theta} = r|_{\theta+\Delta\theta}$ at $\theta = 0$ and $\theta = \pi$, a straight alignment is formed (e.g., Figure 2 (a)). The length ratio of modules' edges at angles 0, $\pi$, $\frac{\pi}{2}$, and $-\frac{\pi}{2}$ determines whether modules dock either back and forth or side by side. For example, the shape shown in Figure 2 (a) has a longer side edge to the major edge ($r|_{\theta=0} < r|_{\theta=\frac{\pi}{2}}$), and the modules assemble back and forth. Whereas the module shown in Figure 2 (b) has a shorter side edge to the main edge ($r|_{\theta=0} > r|_{\theta=\frac{\pi}{2}}$), which causes lateral aggregations. At distant two magnetic modules, since torque dominates force, two distant magnetic modules follow the tendency to first align their magnetic orientations and eventually to collide. Therefore, the edge shapes at $\theta = 0$ and $\theta = \pi$ are considered to be significantly influential in the aggregation.

### 4.1.2 Vertical alignment

Figure 6 (b) describes the geometry of two modules with vertically attached magnets in which two components change relative angles ($\theta_1$, $\theta_2$), while keeping contact. Once the initial contact positions are determined, the shapes of the modules, that can be described with *shape functions*, can be mapped on

the same plot whose x-axis is the common boundaries having experienced a contact (indicated as $u$ in Figure 6 (b)). In this case, the rotation of the modules (in local coordinate) can be predicted by the distance of the two functions. Unless some external turbulence occurs, the convergence (here rotations) should last until the distance reaches the local minimum. The *shape function* reflects the energetic stability of the components.

Take the lattice assembly in Figure 3 (a) as an example: The stability of the formed structures was intrinsically determined by the shape of the constitutive tiles. Rounded tiles induced a folding motion, which was hardly observed in sharp-cornered tiles, enabling the clusters to smoothly converge to further stable states. It is also worth mentioning that bonding strength between modules is commonly reinforced by the component's morphology. Desired bondings make use of shape matching in addition to magnetic pole matching to restrict the bonding condition.

The initial contact positions of two modules can be directed by making one module possess two magnets: one pointing up and one pointing down. In this manner, the counterpart module receives a biased field such that it becomes attracted to the corresponding magnetic side. This indicates the possibility that some guiding mechanisms for an aggregation can be further integrated as morphological properties.

## 4.2 Assembly

### 4.2.1 Emergence and Allostericity

As can be seen in the bike-like configuration in Figure 3 (g), where a combination of three circular modules and a triangular module yields functional mobility, combinations of basic components often exhibit meaningful behavior.

Suppose there are two different modules/clusters: $\mathcal{A}$ and $\mathcal{B}$. In general, interactions of two modules/clusters can be described with combinations of the following three reaction steps:

$$\begin{array}{lcc} \text{(I)} & \text{Forward reaction} & \mathcal{A}+\mathcal{B}\rightarrow\mathcal{AB} \\ \text{(II)} & \text{State change} & \mathcal{A}\rightarrow\mathcal{A}' \\ \text{(III)} & \text{Backward reaction} & \mathcal{AB}\rightarrow\mathcal{A}+\mathcal{B}. \end{array}$$

A state change can be any conformational/internal change inducing the acquisition of another functionality of the module, e.g., conformation change of a protein, protruding a sticking site (charged site) out of the body such that it can react with another protein. In distributed systems, this sort of acquisition of functionality is normally accompanied with combining to another module, and can be described as

$$\begin{array}{lcc} \text{(I)+(II)} & \textit{Allosteric plus} & \mathcal{A}+\mathcal{B}\rightarrow\mathcal{A}'\mathcal{B} \\ \text{(II)+(III)} & \textit{Allosteric minus} & \mathcal{AB}\rightarrow\mathcal{A}'+\mathcal{B}, \end{array}$$

which we termed Allosteric plus and Allosteric minus, respectively. In the *Allosteric plus* reaction, a component connects to another component and eventually obtains a different characteristic. Such an acquisition of functionality spontaneously leads to the next reaction. Note that the reaction order can be sorted through this process, and this is the only way to sort the aggregation sequence in assembly processes. In the *Allosteric minus* reaction, which is the opposite case, a cluster disassembles a part of itself and obtains a different characteristic. In this way, all the reaction processes in a system can be described algebraically, employing causal analysis. In the case of crystal formation in snow flakes, the atoms change their conformation and allow the next atom to attach.

In artificial self-assembly systems utilizing magnets, however, as we saw in Figure 3 (j), (k), having elaborated internal states that enable the component to physically express a/various state(s) is a trade-off in two ways: it leads to vulnerability against environmental turbulence, and it induces overweight of components and hinders rapid motions and structural stability. The benefit of having different types of components compensates for such problems, and eventually guarantees the diversity of reactions, while maintaining the complexity of the causal rule. In other words, fertility in heterogeneity lightens the mechanical load of the components. Finding a suitable level of heterogeneity must become one of the capital issues in artificial self-assembly systems.

Obtaining a functionality as an allosteric effect can be achieved as a combination of a simple set of components, of which we see an example in Figure 2 (f). As the attractive region for the external tiles depends on the configuration of the constitutive tiles, the system differentiates its characteristics through the structure's morphology. The difference between functionality and allostericity is that while the former mainly exerts influence to the system in an analogue manner, the latter operates in a digital way, and its features are mostly distinctive. In addition, an allosteric component is not only capable of playing roles of two different types of components, but also generates various temporal causalities. Heterogeneous systems, which consist of many different types of components, on the other hand, often encounter divergence of the components' combinatorial problems, in which enrolled components regularly yield undesired compounds due to the lack of a reaction's temporal constraint. In this regard, parallelism is another keyword that describes the characteristics of stochastic self-assembly.

### 4.2.2 Parallelism

Unlike conventional multi-tasking assembly systems, self-assembly systems deal with multi-degree parallelism in their assembly processes. Parallelism occurs not only in the spatial dynamics, but also along a temporal dimension, where the progress of different stages of reactions can be observed simultaneously. Such as we established in one of the prerequisites in the logical model shown in Figure 2 (j) (k), most of our systems suppose magnetic attractions between desired attachments and either repulsions or no relation between undesired attachments. This postulate prevents the system from further extension in

the diversity in the type of components, and hence, in the complexity of reaction paths. In this respect, templation plays a role of not only spatially sorting the dynamics but also temporarily coordinating the assembly.

As for a solution for quantitative measure, we previously proposed a measuring method of *degree of parallelism* ($H$) in self-assembly processes (Miyashita et al., 2009b). Let $c_i$ be the factor of clustering degree of a cluster $i$ ($i \in N$), which is defined as:

$$c_i = \frac{\text{number of connections within the } i\text{-th cluster}}{\text{number of connections within the complete configuration}}. \tag{5}$$

The $H$ can be defined as:

$$H = -\sum_{i=1}^{N} c_i \ln c_i, \tag{6}$$

which takes various values between 0 and 1 over an assembly process. The higher the value is, more in parallel that the assembly process proceeds.

## 4.3 Environment

### 4.3.1 Stochasticity

Our system exploits magnetic attraction as a long-range interactive force. Boncheva *et al.* pointed out the rare uses of magnetism in biology for self-assembly, although the solutions derived in nature may not be optimal when using non-biological components (Boncheva and Whitesides, 2005). In molecular assembly, three conditions are known to be necessary: weak interaction, thermal agitation, and nucleation. The mechanism behind molecular assembly is numerous trial and error iterations of the connections until the connection strength reaches a sustainable level, which is beyond the pressure of proofreading through environmental turbulence. It utilizes environmental diffusion as a traveling aid and achieves highly efficient assembly matching per unit time. Through such a process, the system gradually shifts to a more energetically stable state. This is one of the fundamental differences from pick-and-place style (deterministic) assembly in engineering.

As for a quantitative measure representing a time-scale dependency, the Reynolds number $\mathcal{R}_\mathbf{e}$, that describes the ratio between viscous forces and inertial forces for a particle traveling through liquid, is often referenced (Purcell, 1977);

$$\mathcal{R}_\mathbf{e} \equiv \frac{\text{inertial forces}}{\text{viscous forces}} \approx \frac{av\rho}{\mu}. \tag{7}$$

where $a$ is the characteristic distance (e.g., radius of a particle), $v$ is the speed of the particle, $\mu$ is the fluid dynamic viscosity, and $\rho$ is the fluid density. Due to $a$ and $v$, biological systems in the $nm - \mu m$ scale are known to often show unique behaviors that cannot be observed in larger scales. This is partially due to the influence of viscosity, which becomes increasingly dominant with decreasing length scales. For

objects on the order of $1\,\mu\,m$ or less, exploiting an environmental diffusion is often a more effective way of locomotion than active propulsion. For example, Purcell states the efficiency of creatures in small scale ($\mu m$) such as E. coli to use diffusion through their environment to change their position, rather than self-propelling (Purcell, 1977).

In contrast, objects larger than $10\,mm$ under water are affected more by inertial forces than viscous forces (environment in high $Re$). In our system, due especially to this inertial effect, the frequency of collisions has a practical limit. This low capacity for collision-matching of macroscopic self-assembly invokes a demand for accurate bondings and the need for long-range instructions that lead to accurate alignments in the bonding processes. This provides us with a strong argument that utilizing small-sized magnets is preferable. The designed component architecture leaves open the possibility of system scalability, ideally for miniaturization. In addition, instead of using vibration motors, a similar agitation could be realized by externally applying a rotational magnetic field (or physical turbulence), expected to induce torque on the modules' magnets. However, this cannot be perfect local agitation. The demand for self-agitation may arise for this reason.

At the molecular level, if the system has a constant temperature and a pressure, Gibbs free energy defines the change of free energy ($\Delta G$). The $\Delta G$ is given by the combination of change of the Enthalpy ($\Delta H$) and the Entropy ($\Delta S$), namely

$$\Delta G = \Delta H - T\Delta S, \tag{8}$$

where $T$ is the temperature of the system. The Enthalpy is the sum of the internal energy as well as the work produced by the system (in our system, mainly bonding energy or magnetic potential energy, and kinetic energy) (Moore et al., 2004). An entropic effect, often termed depletion force, plays an increasingly important role as the length of the scale decreases (e.g. the self-assembly of lipid phases is almost exclusively driven by entropic effects). The fact that entropic effects can be neglected at macroscopic scales is connected to the fact that the bigger the scale the smaller the (relative) fluctuations.

#### 4.3.2 2D vs. 3D

It is suggested that self-assembly is the only practical way to manipulate and order nano- and micrometer-sized components into 3D structures (Boncheva and Whitesides, 2005). As introduced in Section 1, many studies have carried out assembly processes on 2D platforms (Pawashe et al., 2009). The distinction between a 2D model and a 3D model is not as trivial as it may seem at first glance. Normally a component has six degrees of freedom (DOF) $(X, Y, Z, Roll(\phi), Yaw(\theta), Pitch(\psi))$ in 3D space. Here, we distinguish two types of 2D:

$$2\mathrm{D_I} \quad \mathrm{DOF} \quad = \quad (x, y, \phi, \theta, \psi) \tag{9}$$

$$2\mathrm{D_{II}} \quad \mathrm{DOF} \quad = \quad (x, y, \theta) \tag{10}$$

The $2D_I$ allows a component to rotate in 3D on a 2D plane, while $2D_{II}$ does not (the movement of components is restricted to a 2D plane).

Table 3 summarizes the differences between 2D and 3D in self-assembly.

[Table 3]

1. **Difference on components supply** The difference is noticeable. The supply path is affected by the configuration of the structure in 2D models (*dead end problem*), i.e., some part of the structure may become unreachable. This has less influence on 3D structures.
2. **Difference on physical interaction** A component in $2D_I$ can interact with another component on the plane as if it were in 3D[1]. Whereas in $2D_{II}$, interactions among components is restricted to the 2D plane.
3. **Difference on product structure** Exceptions may be components that possess flexibility and fold (such as proteins).

In general, if the aim is to construct 3D structures, $2D_I$ may provide a sufficient solution, whereas if the aim is to cover the space, the system needs to be extended to 3D.

# 5 Conclusion

This study discusses various features attributed to magnetic two- dimensional self-assembling systems, aiming to highlight the design principles of highly autonomous self-assembly systems that are applicable to different scales. We first elucidated that the form of magnet alignment characterizes the assembly patterns. For instance, when magnets are attached horizontally to each module, the module shows aspects of a dipole. On the other hand, if magnets are attached vertically, each module behaves as a monopole. We further examined the attributes from different perspectives: reaction, product, magnetic flux, structural isomer, functionality, controllable parameter, dynamics, and self-repair. Through case studies, the elucidated features gave rise to unique insights into the interdependencies between the components' morphologies, the systems' stochasticity, and the complexity of the assembly paths, which, we believe, deepens the understanding of self-assembly systems.

# Acknowledgment

This work was partially supported by a Swiss National Science Foundation Fellowship PBZHP2-133472.

[1] for sufficiently large distances between the components

# References


Audretsch, C. (2009). Development of a sensing system for detecting the neighbour in self-assembly robots. Master's thesis, Julius-Maximilians-Universitt Würzburg.

Bishop, J., Burden, S., Klavins, E., Kreisberg, R., Malone, W., Napp, N., and Nguyen, T. (2005). Programmable parts: A demonstration of the grammatical approach to self-organization. In *IEEE/RSJ International Conference on Intelligent Robots and Systems (IROS)*, pages 3684–3691.

Boncheva, M., Andreev, S. A., Mahadevan, L., Winkleman, A., Reichman, D. R., Prentiss, M. G., Whitesides, S., and Whitesides, G. (2005). Magnetic self-assembly of three-dimensional surfaces from planar sheets. *PNAS*, 102:3924–3929.

Boncheva, M., Ferrigno, R., Bruzewicz, D. A., and Whitesides, G. M. (2003). Plasticity in self-assembly: Templating generates functionally different circuits from a single precursor. *Angewandte Chemie International Edition*, 42:3368–3371.

Boncheva, M., Gracias, D. H., Jacobs, H. O., and Whitesides, G. M. (2002). Biomimetic self-assembly of a functional asymmetrical electronic device. *PNAS*, 99:4937–4940.

Boncheva, M. and Whitesides, G. M. (2005). Making things by self-assembly. *MRS BULLETIN*, 30:736–742.

Bowden, N., Terfort, A., Carbeck, J., and Whitesides, G. M. (1997). Self-assembly of mesoscale objects into ordered two-dimensional arrays. *Science*, 276:233–235.

Bowden, N., Weck, M., Choi, I. S., and Whitesides, G. M. (2001). Molecule-mimetic chemistry and mesoscale self-assembly. *Accounts of Chemical Research*, 34:231–238.

Breivik, J. (2001). Self-oranization of template-replicating plolymers and the spontaneous rise of genetic information. *Entropy*, 3:273–279.

Cohn, M. B. and Kim, C.-J. (1991). Self-assembling electrical networks: An application of micromachining technology. In *International Conference on Solid-State Sensors and Actuators*.

Gilpin, K., Knaian, A., and Rus, D. (2010). Robot pebbles: One centimeter module for programmable matter through self-disassembly. In *IEEE International Conference on Robotics and Automation*.

Gracias, D. H., Tien, J., Breen, T. L., Hsu, C., and Whitesides, G. M. (2000). Forming electrical networks in three dimensions by self-assembly. *Science*, 289:1170–1172.

Griffith, S., Goldwater, D., and Jacobson, J. (2005). Robotics: Self-replication from random parts. *Nature*, 437:636.

Gross, R. and Dorigo, M. (2008). Self-assembly at the macroscopic scale. *Proceedings of the IEEE*, 96:1490–1508.

Grzybowski, B. A., Radkowski, M., Campbell, C. J., Lee, J. N., and Whitesides, G. M. (2004). Self-assembling fluidic machines. *Applied physics letters*, 84:1798–1800.

Grzybowski, B. A., Stone, H. A., and Whitesides, G. M. (2000). Dynamic self-assembly of magnetized, millimetre-sized objects rotating at a liquid-air interface. *Nature*, 405:1033.

Grzybowski, B. A., Winkleman, A., Wiles, J. A., Brumer, Y., and Whitesides, G. M. (2003). Electrostatic self-assembly of macroscopic crystals using contact electrification. *Nature Materials*, 2:241–245.

Hosokawa, K., Shimoyama, I., and Miura, H. (1994). Dynamics of self-assembling systems: Analogy with chemical kinetics. *Artificial Life*, 1(4):413–427.

Klavins, E. (2007). Programmable self-assembly. *IEEE Control System Magazine*, 27:43–56.

Mao, C., Thalladi, V. R., Wolfe, D. B., Whitesides, S., and Whitesides, G. M. (2002). Dissections: Self-assembled aggregates that spontaneously reconfigure their structures when their environment changes. *J. Am. Chem. Soc*, 124(49):14508 –14509.

Miyashita, S. (2011). *Effect of Morphology on Scalable Self-Assembling Robots in Pursuit of Living Artificial Systems*. PhD thesis, University of Zurich.

Miyashita, S., Casanova, F., Lungarella, M., and Pfeifer, R. (2008a). Peltier-based freeze-thaw connector for waterborne self-assembly systems. In *IEEE/RSJ International Conference on Intelligent Robots and Systems (IROS)*, pages 1325–1330, Nice, France.

Miyashita, S., Göldi, M., and Pfeifer, R. (2011). How reverse reactions influence the yield rate of stochastic self-assembly. *International Journal of Robotics Research*, 30:627 – 641.

Miyashita, S., Kessler, M., and Lungarella, M. (2008b). How morphology affects self-assembly in a stochastic modular robot. In *IEEE International Conference on Robotics and Automation (ICRA)*, pages 3533–3538, Pasadena, USA.

Miyashita, S., Lungarella, M., and Pfeifer, R. (2009a). *Artificial Life Models in Hardware*, chapter Tribolon: Water Based Self-assembly Robot, pages 161–184. Springer, ISBN: 978-1-84882-529-1 edition.

Miyashita, S., Nagy, Z., Nelson, B. J., and Pfeifer, R. (2009b). The influence of shape on parallel self-assembly. *Entropy*, 11:643–666.

Moore, J. W., Stanitski, C. L., and Jurs, P. C. (2004). *Chemistry: The Molecular Science*. Brooks Cole.

Pawashe, C., Floyd, S., and Sitti, M. (2009). Magnetic mobile micro-robots. In *7ème Journées Nationales de la Recherche en Robotique*.

Penrose, L. S. (1958). Mechanics of self-reproduction. *Annals of Human Genetics*, 23:59–72.

Penrose, L. S. (1959). Self-reproducing. *Scientific American*, 200-6:105–114.

Purcell, E. M. (1977). Life at low reynolds number. *American Journal of Physics*, 45:3–11.

Saitou, K. (1999). Conformational switching in self-assembling mechanical systems. *IEEE Transactions on Robotics and Automation*, 15:510–520.

Saitou, K. and Jakiela, M. J. (1995a). Automated optimal design of mechanical conformational switches. *Artificial Life*, 2:129–156.

Saitou, K. and Jakiela, M. J. (1995b). Subassembly generation via mechanical conformational switches. *Artificial Life*, 2:377–416.

Saitou, K., Wang, D.-A., and Wou, S. J. (2000). Externally resonated linear microvibromotor for microassembly. *Journal of Microelectromechanical Systems*, 9:336–346.

Stambaugh, J., Lathrop, D. P., Ott, E., and Losert, W. (2003). Pattern formation in a monolayer of magnetic spheres. *Pysical Leview E*, 68:026207–1–026207–5.

Tolley, M. T. and Lipson, H. (2010). Fluidic manipulation for scalable stochastic 3d assembly of modular robots. In *IEEE International Conference on Robotics and Automation*.

Tsutsumi, D. and Murata, S. (2007). Multistate part for mesoscale self-assembly. In *SICE Annual Conference*, pages 1–6.

White, P., Kopanski, K., and Lipson, H. (2004). Stochastic self-reconfigurable cellular robotics. In *IEEE International Conference on Robotics and Automation (ICRA)*, pages 2888–2893.

White, P., Zykov, V., Bongard, J., and Lipson, H. (2005). Three dimensional stochastic reconfiguration of modular robots. In *International Conference on Robotics Science and Systems (RSS)*, pages 161–168.

Wolfe, D. B., Snead, A., Mao, C., Bowden, N. B., and Whitesides, G. M. (2003). Mesoscale self-assembly: Capillary interactions when positive and negitive menisci have similar amplitudes. *Langmuir*, 19(6):2206–2214.

Yamaki, M., Higo, J., and Nagayama, K. (1995). Size-dependent separation of colloidal particles in two-dimensional convective self-assembly. *American Chemical Society*, 11:2975–2978.

Yokoi, H., Nagai, T., Ishida, T., Fujii, M., and Iida, T. (2003). *Morpho-functional Machines: The New Species: Designing Embodied Intelligence*. Springer.

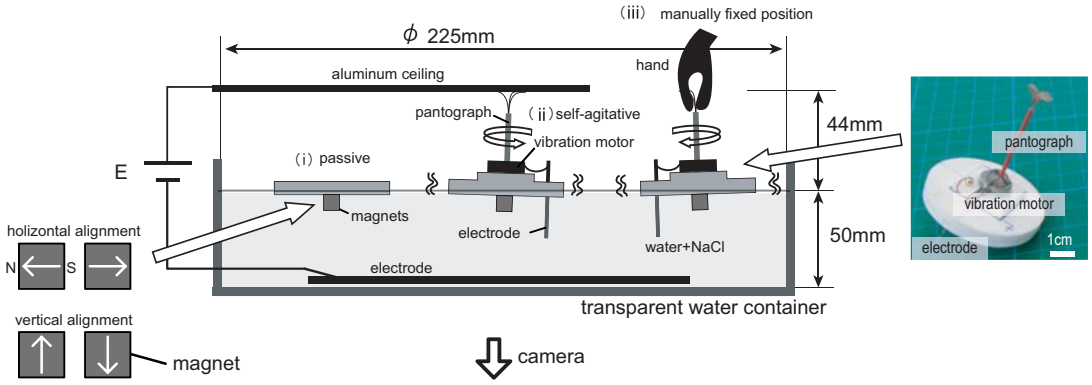


**Figure 1:** General experimental setup. Three modules from left to right; passive, self-agitative, and manually constraint. Self-agitative module weighs $2.8\,g$ and has a footprint of $12.25\,cm^2$.

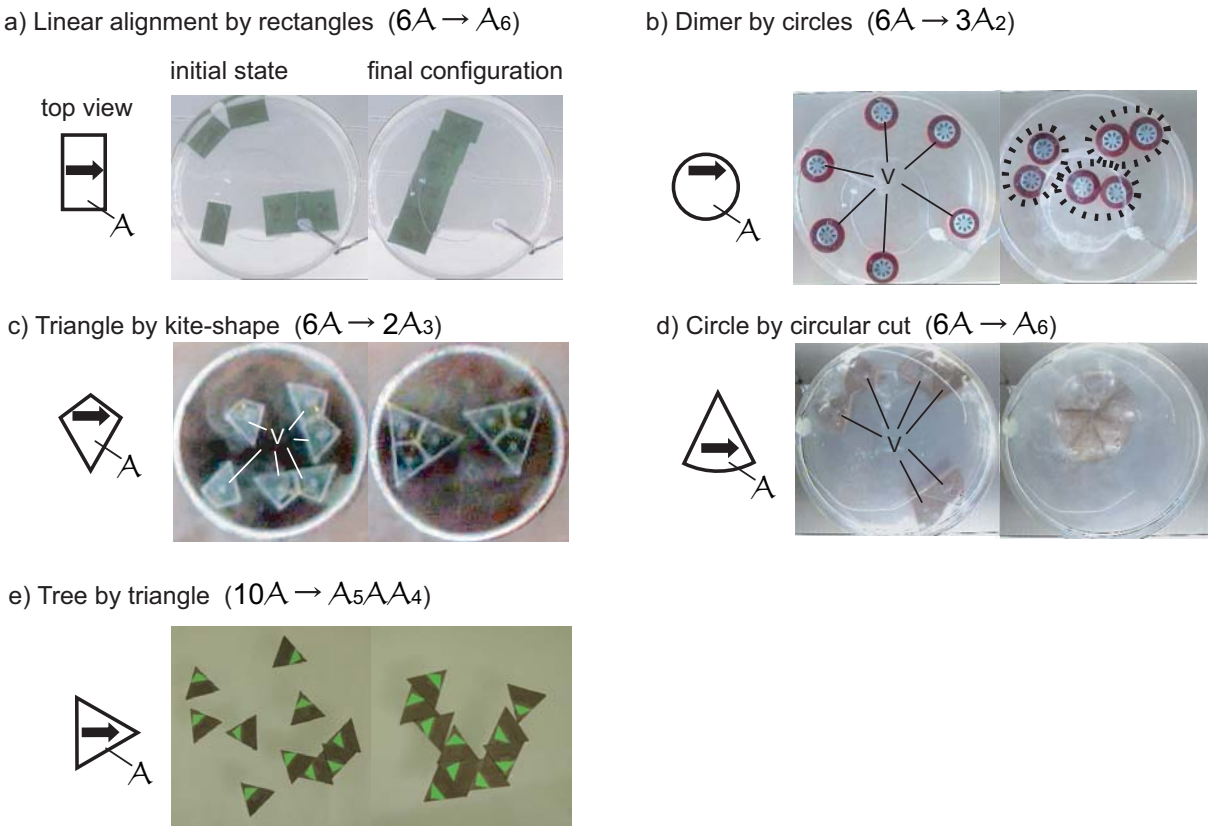


**Figure 2:** The assembly patterns of different modules that are equipped with horizontally aligned magnets: linear alignment (a) (Miyashita et al., 2009a), clustering (b-d) (Miyashita et al., 2009a, 2008a,b), and tree (e). The modules containing vibration motors are indicated with the letter "V".E The arrows in each illustration represent the way in which the magnets are attached. Each reaction is described with a chemical formula. Note that the same $\mathcal{A}$ in different examples shows different types of modules.

f) Lattice by passive squares ($10A+10B \rightarrow (AB)_{10}$)

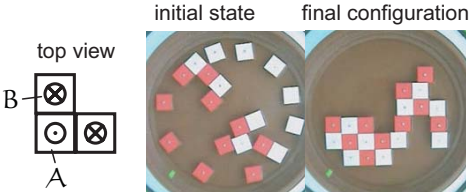


g) Mobility by vibrating triangle and circles ($3A+B \rightarrow A_3B$)

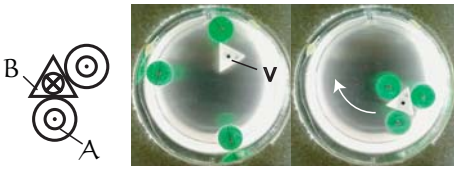


h) Concentric circle by vibrating and passive circles ($A_2B+A \rightarrow A_3B$)

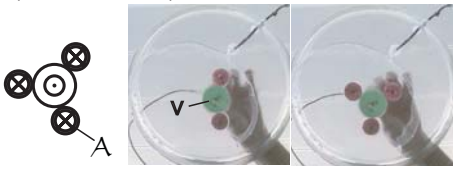


i) Gear by vibrating triangle and circles ($A_2B+2A+2B \rightarrow (AB)_3$)

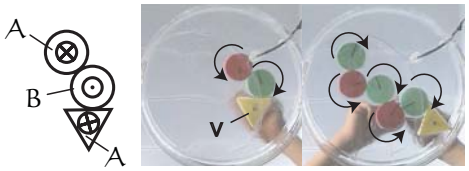


j) Enzyme reaction by passive modules ($A+BC \rightarrow A+B'+C$)

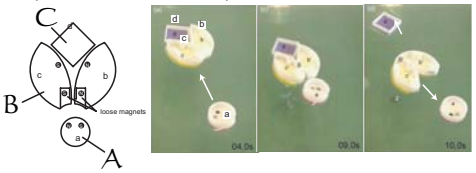


k) Disassembly by passive modules ($2A+B \rightarrow A+AB$)

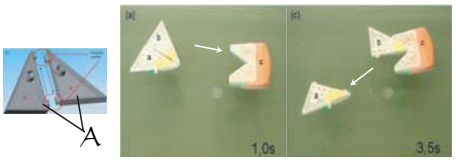


**Figure 3:** The assembly patterns of modules with vertically aligned magnets. The modules containing vibration motors are indicated by the letter "V."E Lattice by passive squares (f) (Miyashita et al., 2009b); Mobility by vibrating triangle and circles (g) (Miyashita, 2011); Concentric circle by vibrating and passive circles (h) (Miyashita et al., 2009a); Gear by vibrating triangle and circles (i) (Miyashita et al., 2009a); Logical enzyme reaction (j) (Audretsch, 2009); Disassembly by passive third module (k) (Audretsch, 2009). Each reaction is described with a chemical formula.

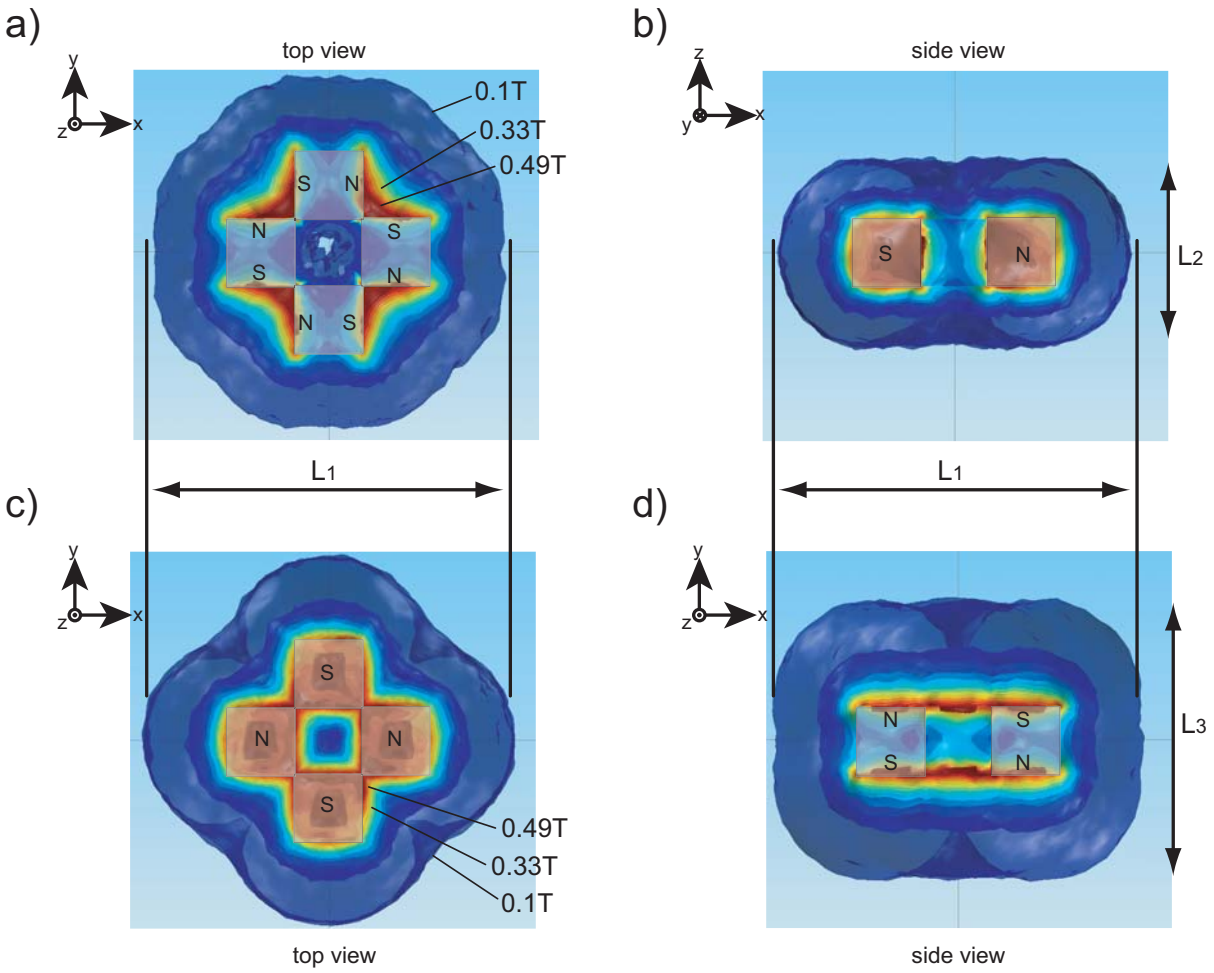


**Figure 4:** Figure 4 shows the distribution of the norms of magnetic flux density ($||B||$. We set the magnetization of each module as 750 [kA/m]) when aligning four magnets horizontally (top view in (a) and side view in (b)), and vertically (top view in (c) and side view in (d)) in lattice structures. The norms of magnet flux density spread similarly in horizontal directions (indicated as $L1$), and spread differently in vertical directions ($L2 < L3$).

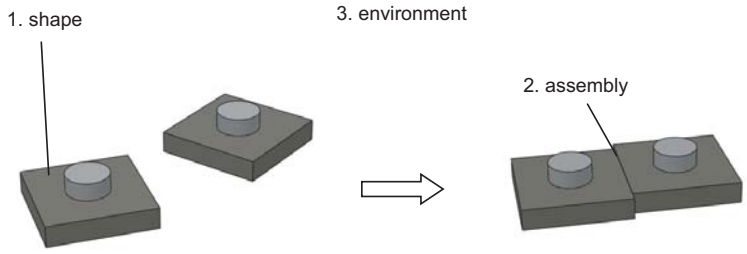


**Figure 5:** Three perspectives on a magnet-driven self-assembly system.

a) horizontal alignment

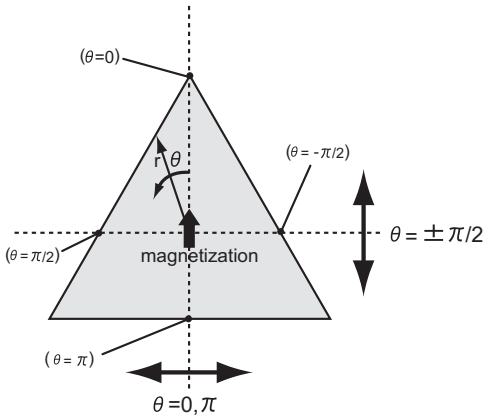


b) vertical alignment

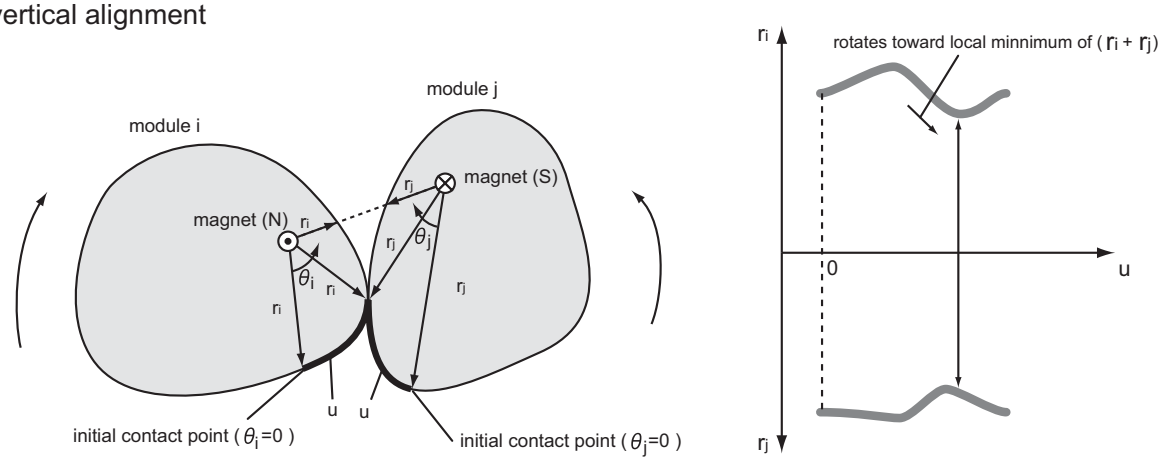


**Figure 6:** Evaluation of the shapes of modules with (a) a horizontally attached magnet and (b) a vertically attached magnet.

**Table 1:** Attributes of the systems shown in Figure 2 and Figure 3 a to k.

| | Magnets Attachment | 1) Reaction | 2) Product | 3) Magnetic flux | 4) Structural isomer | 5) Functionality | 6) Controllable parameter | 7) Dynamics | 8) Self-repair |
|---|---|---|---|---|---|---|---|---|---|
| (a) | horizontal | $6\mathcal{A} \rightarrow \mathcal{A}_6$ | linear polymer | open | none[a] | - | - | static | possible |
| (b) | horizontal | $6\mathcal{A} \rightarrow 3\mathcal{A}_2$ | dimer | closed | none | - | - | dynamic | possible |
| (c) | horizontal | $6\mathcal{A} \rightarrow 2\mathcal{A}_3$ | trimer | closed | (exist)[b] | - | - | dynamic | possible |
| (d) | horizontal | $6\mathcal{A} \rightarrow \mathcal{A}_6$ | hexamer | closed | (exist)[b] | - | - | dynamic | possible |
| (e) | horizontal | $10\mathcal{A} \rightarrow \mathcal{A}_5\mathcal{A}\mathcal{A}_4$ | tree | open | exist | - | - | static | possible |
| (f) | vertical | $10\mathcal{A} + 10\mathcal{B} \rightarrow (\mathcal{A}\mathcal{B})_{10}$ | 2D lattice | open | exist | - | - | static | possible |
| (g) | vertical | $3\mathcal{A} + \mathcal{B} \rightarrow \mathcal{A}_3\mathcal{B}$ | concentric circle | open | (exist)[b] | mobility | translational speed | dynamic | possible |
| (h) | vertical | $\mathcal{A}_2\mathcal{B} + \mathcal{A} \rightarrow \mathcal{A}_3\mathcal{B}$ | concentric circle | open | (exist)[b] | - | rotational speed | dynamic | possible |
| (i) | vertical | $\mathcal{A}_2\mathcal{B} + 2\mathcal{A} + 2\mathcal{B} \rightarrow (\mathcal{A}\mathcal{B})_3$ | polymer | open | exist | torque transformation | transferred rotational speed | dynamic | possible |
| (j) | vertical | $\mathcal{A} + \mathcal{B}\mathcal{C} \rightarrow \mathcal{A} + \mathcal{B}' + \mathcal{C}$ | - | open | - | allostericity | - | static | difficult |
| (k) | vertical | $2\mathcal{A} + \mathcal{B} \rightarrow \mathcal{A} + \mathcal{A}\mathcal{B}$ | - | open | - | allostericity | - | static | difficult |

[a] strictly speaking structural isomer exists by facing the short edges side by side, but can be minimized by regulating the agitation level and the shape.

[b] if more modules exist

**Table 2:** Pros and cons for horizontal/vertical alignment.

| | Horizontal alignment | Vertical alignment |
|---|---|---|
| pros | strong torque employment<br>easy to close the flux | repulsive force employment<br>easy to design architectures |
| cons | difficult to introduce repulsive force<br>difficult to design architectures | no torque to employ<br>difficult to close the flux |

**Table 3:** The difference between 2D vs. 3D in "3D" world

| | component's supply | physical interaction | producible structure |
|---|---|---|---|
| $2D_I$ | *dead end problem* | **close to 3D** | **quasi-3D** |
| $2D_{II}$ | *dead end problem* | constrained | 2D |
| 3D | easier than 2D | 3D | 3D |